Scientiae Radices, **1**, 3-25 (2022)

Review

In memory of the first historical president of Radom Scientific Society (RTN), Dr. Stefan Witkowski

SciRad SCIENTIAE RADICES

2D Metal Halide Perovskites: A New Fascinating Playground for Exciton Fine Structure Investigations

Michał Baranowski[1], Mateusz Dyksik[1], Paulina Płochocka[1,2] ✉

(1) Department of Experimental Physics, Faculty of Fundamental Problems of Technology, Wroclaw University of Science and Technology, 50-370 Wroclaw, Poland
(2) Laboratoire National des Champs Magnétiques Intenses, EMFL, CNRS UPR 3228, Université Grenoble Alpes, Université Toulouse, Université Toulouse 3, INSA-T, Grenoble and Toulouse, France

✉ Correspondence to: paulina.plochocka@lncmi.cnrs.fr

Abstract: Two-dimensional (2D) metal halide perovskites are natural quantum wells which consist of low bandgap metal-halide slabs, surrounded by organic spacers barriers. The quantum and dielectric confinements provided by the organic part lead to the extreme exciton binding energy which results in a huge enhancement of exciton fine structure in this material system. This makes 2D perovskites a fascinating playground for fundamental excitonic physics studies. In this review, we summarize the current understanding and quantification of the exciton fine structure in 2D perovskites. We discuss what is the role of exciton fine structure in the optical response of 2D perovskites and how it challenges our understanding of this fundamental excitation. Finally, we highlight some controversy related to particularly large bright-dark exciton states splitting and high efficiency of light emission from these materials. This can result from the unique synergy of excitonic and mechanical properties of 2D perovskites crystals.

Keywords: 2D perovskites, exciton, fine structure, dark exciton states

Received: 2022.08.30
Accepted: 2022.10.13
Published: 2022.11.18
DOI: 10.58332/v22i1a01

Introduction

Despite being known for more than 100 years, organic-inorganic perovskites have recently emerged as revolutionary materials for lighting and energy harvesting applications. The unprecedented potential of organic-inorganic lead halide perovskites results from a unique combination of their optoelectronic and mechanical properties [1]. They exhibit strong broadband absorption [2,3], together with a long carrier lifetime, diffusion length [2] and defect tolerance [4,5], which makes them almost ideal materials for photovoltaic application. Unfortunately, the intense investigation of bulk (3D) metal halide perovskite highlighted their intrinsic instability to moisture, which directed the interest of the scientific community toward different, more stable, members of the perovskites family, such as 2D layered perovskites [6-8]. Besides maintaining good performance in photovoltaic and light-emitting applications [6-11] 2D perovskites exhibit supreme tunability of their optical properties [7,12,13] in comparison with their 3D counterparts.

In parallel to the great potential in real-life applications, 2D perovskites also constitute a fascinating playground for fundamental excitonic physics studies, where the unique synergy of soft lattice and optoelectronic properties challenges our understanding of this elementary optical excitation [1,11,14]. Despite intensive investigations, many fundamental questions about exciton physics remain unanswered in the case of 2D perovskites. Here in this article, we revise the current understanding and open questions related to the exciton physics in 2D perovskites with special attention devoted to the exciton fine structure and its role in the surprising light emission efficiency.

2D perovskites

Metal-halide perovskites are ionic crystals, characterized by AMX_3 structure, shown in Figure 1. In the AMX_3 structure A is typically an organic cation, e.g., A = $CH_3NH_3^+$= MA (MethylAmmonium) or A =$CH(NH_2)_2$= FA (FormAmidinium) or inorganic Cs^+, while M = Pb^{2+}, Sn^{2+} and X = Cl^-, I^- or Br^-. The metal cation (M) is situated inside the halide (X) octahedral cage. The octahedra join via corners and the space between them is filled with the organic or inorganic A cation. As a consequence of its ionic nature perovskite crystal lattice is around 10 times softer than conventional (covalent) semiconductors which has an important impact on the optoelectronic properties of these semiconductors [1,14,15].

The 2D perovskite structure can be conceptually derived from the corresponding 3D crystal. For example, in the case of $MAPbI_3$, the crystal structure consists of PbI_6^4 octahedra

forming a layer interconnected to other layers via the halogen atom sites with the space between neighboring octahedral cages filled by small methylammonium cations. The incorporation of larger organic cation spreads the 3D perovskite structure into slabs, which are separated by long organic chains [7,11] (schematically presented in Figure 2b). By changing the stoichiometry of long and small organic cations, it is possible to tune the thickness of the inorganic slab [16]. The layered structures can be divided into two categories: Ruddlesden-Popper (RP) [7] phase with general formula $A'_2A_{n-1}M_nX_{3n+1}$, and Dion-Jacobson (DJ) [12] phase described by $A'A_{n-1}MnX_{3n+1}$. A' is 1^+ or 2^+ organic spacer cation for example phenylethylammonium (PEA) or Butylammonium (BA) for RP or 3-(aminomethyl)piperidinium (3AMP) or 4-(amino-methyl)piperidinium for DJ phase, A is a 1^+ cation (MA, FA, Cs, EA, GUA), and M can be Pb^{2+}, Sn^{2+}, Ge^{2+}, Cu^{2+}, Cd^{2+}, etc., X = Cl^-, Br^-, I^- and n=1,2,3... is the number of octahedra in the inorganic slab. In the further part of the article, we will focus on the RP phase since the DJ phase is much less investigated.

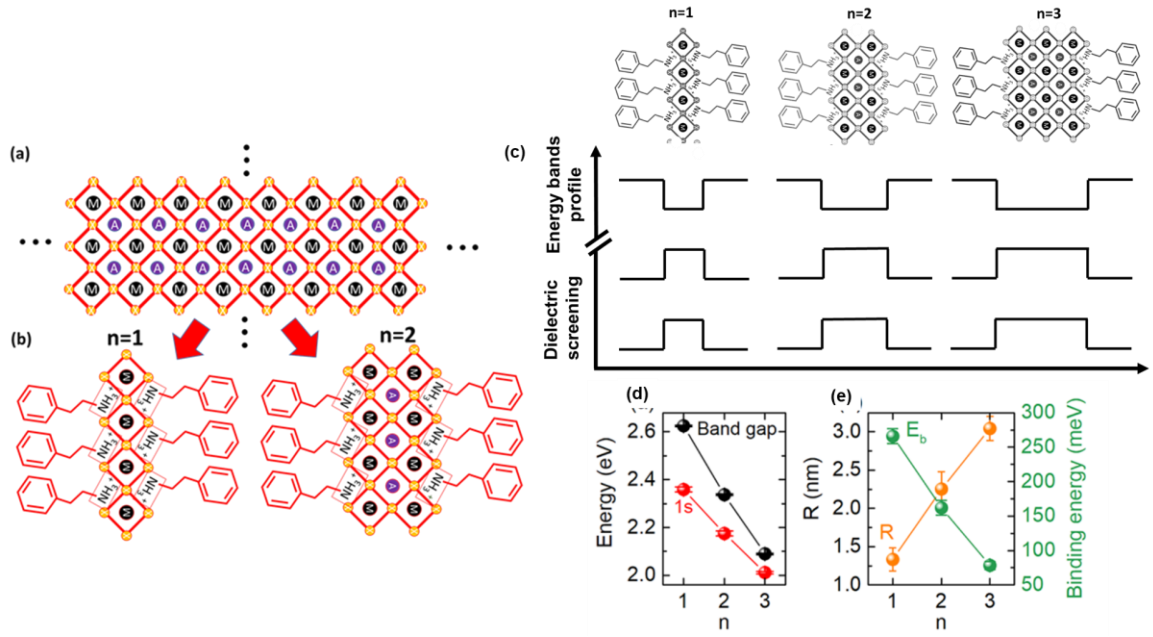

Fig. 1. (a) Schema of the 3D perovskite structure (b) 2D perovskite structure for n=1 and n=2 in in Ruddlesden-Popper pahse. M stand for metal cation (Pb^{2+}, Sn^{2+}), X is a halide anion (I^-, Br^-, Cl^-) and A is a cation situated in the voids between octahedral (MA, FA, or Cs^+). (c) Schematics of 2DPs of different thicknesses (indicated by n) together with the spatial profiles of conduction and valence bands and dielectric screening. (d) The energy of ground exciton state and single-particle band gap as a function of n for $(PEA)_2MA_{n-1}Pb_nI_{3n-1}$. (where PEA stands for phenylethylammonium) (e) Exciton binding energy and exciton radius as a function of n for $(PEA)_2MA_{n-1}Pb_nI_{3n-1}$. Panel (d) and (e) reprinted with permission from [17] Copyright 2021 American Chemical Society.

The presence of organic spacers provides extra knobs to tune the properties of 2D perovskites in addition to well-known for other quantum well (QW) systems methods of chemical composition or quantum well width modifications [11,18,19]. The length and cross-section of the organic spacers determine the distortions of the octahedral units in the soft

inorganic part of QW (which is called templating effect) modifying band structure and vibrational properties of the lattice [19-24]. Since there are a plethora of organic molecules which can be used as spacers [7], this provides a very convenient way to tune electronic properties such as bandgap, exciton binding energy or effective mass of carriers [17,19,20,22,25].

Excitons in 2D perovskites

2D perovskites are often regarded as natural quantum wells, not plagued by interface roughness or intermixing characteristics of epitaxially grown quantum wells. The wells consist of planes of lead-halide octahedra, as shown schematically in Figure 1c, while the barriers are formed by the organic spacers. This basic structure is periodic in the out-of-the-plane direction, with a typical type I band alignment between the inorganic well and the organic spacers [11,26]. In addition to quantum confinement, the significant difference between dielectric constants of the organic spacers and the inorganic slabs (see examples in Table 1) results in dielectric confinement [11,18,25,27-30]. Both types of confinement increase the exciton binding energy far more than in fully inorganic quantum well systems (for example GaAs/AlGaAs) or theoretical 2D limit (a four-fold increase of exciton binding energy), reaching typical values of a few hundred of meV [17,18,29,31]. Therefore, the optical properties of these materials are dominated by excitons even at room temperature. Like in other QW systems when the thickness of the QW well increases both the exciton binding energy and bandgap decrease while the exciton radius increases [17,18] as shown in Figure 1d and 1e.

Table 1. Examples of high-frequency dielectric constants of QW and barriers of a few representatives of 2D perovskites together with exciton binding energy.

	ε_w	ε_b	E_X (meV)
$(PEA)_2PbI_4$	6.1 [32]	3.3 [32]	190 [33] 200 [34] 260 [22] 310 [32]
$(PEA)_2SnI_4$	5.19	3.3	174 [18]
$(PEA)_2PbBr_4$	6.1	3.3	450
$(BA)_2PbI_4$	4.0 [18]	2.1 [18]	370 [35] 470 [18]

Like in any other semiconductor, excitonic states are affected by the exchange interaction between the spins of the electron and hole which leads to the so-called fine structure splitting (FSS) [36-40]. Exchange interaction lifts the degeneracy of the states with different angular momenta (different electron and hole spin configurations). The induced spacing of the excitonic states might have a dramatic impact on the optical properties of materials [41-42]. For example, the low-lying dark exciton states can be an effective channel for nonradiative recombination, while bright state splitting is crucial for single photon sources, or entanglement photon sources [43,44]. The detailed excitonic energetic order in 2D perovskite results from a characteristic, "inverted" band structure (with the conduction band predominantly built from p-like states and valence band states composed of s-type orbitals). Due to strong spin-orbit interaction and crystal field the degeneracy of electron states with respect to angular momentum is lifted and states at the bottom of the conduction band are characterized by a total angular momentum 1/2, the same as holes at the top of the valence band [30,38,45]. Therefore, band-edge excitons are built from electrons and holes, both characterized by a total angular momentum of 1/2. As a result, there are four excitonic states (as shown in Figure 2) characterized by a different total (J=0 or 1) and z-component (J_z=0 or ±1) of angular momentum.

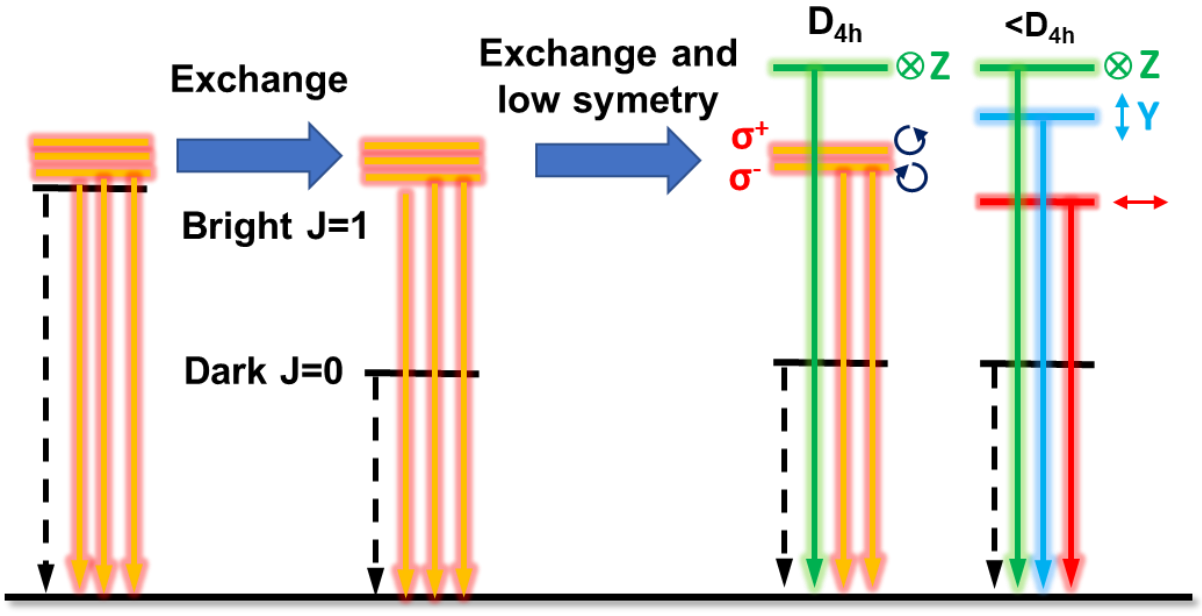

Fig. 2. Evolution of the exciton state structure with exchange interaction and symmetry of 2D perovskites. In D_4h the two in-plane states (orange) are circularly polarized and are eigenstate of J_z operator with eigenvalue ±1. In lower symmetry case the two in plane states are superposition of circularly polarized states and therefore they have linear polarization. In typical experimental configurations the optical response comes from the in-plane state.

The degeneracy between dark singlet (J=0) and bright triplet states (J=1) is always lifted by the exchange interaction and the dark state becomes the ground state, while three optically active states lie at higher energies. In a quantum well-like system, the lack of symmetry in the z-direction further lifts the degeneracy of J=1 states, which results in two degenerate states with $J_z = \pm 1$ and one $J_z = 0$. The pair of degenerate states have a dipole moment in the xy plane of the crystal and couples to left- or right-handed circularly polarized light, while the non-degenerate state has a dipole moment perpendicular to the metal-halide octahedral plane (see Figure 2). In the case of broken in-plane symmetry, the degeneracy of the triplet states is completely lifted and new in-plane states couple to linearly polarized light along x or y direction [38,46]. Since the exciton in 2D perovskites is very tightly bound the exchange interaction is strongly enhanced [36] which results in significant splitting of the excitonic states, far more than in conventional (epitaxial) low dimensional systems. For example, according to available reports, the bright-dark exciton state splitting can reach the value of tens of millielectronvolts for the thinnest perovskite quantum wells [47-50]. This is one or two orders of magnitude larger than in epitaxial structures or nanocrystals [36,37,42,51]. This large splitting, together with all available methods of band structure and confinement engineering makes 2D perovskites potentially an excellent platform for the investigation of exciton FSS physics. However, despite intensive optical studies and all advantages of 2D perovskites, the detailed exciton structure still awaits precise quantification and understanding of how it can be controlled. For example, so far reported bright-dark exciton splitting varies strongly even for nominally the same materials, spanning the range from 4 to 30 meV, which is summarized in Table 2.

Table 2. Summary of reported bright dark states splitting together with the used method (PL - temperature dependent PL spectroscopy, Magnetic field - optical spectroscopy in magnetic field), for different 2D perovskites of thickness n=1.

Methods	$(PEA)_2SnI_4$	$(PEA)_2PbI_4$	$(BA)_2PbI_4$	$(PEA)_2PbBr_4$	$(BA)_2PbBr_4$
PL	10 meV [50]	10 meV [49]	4meV [52]	—	30 meV [48]
Magnetic field	18 meV [47]	22 meV [47] 16 meV [53]	—	27meV [47]	—

Determination of dark bright state splitting

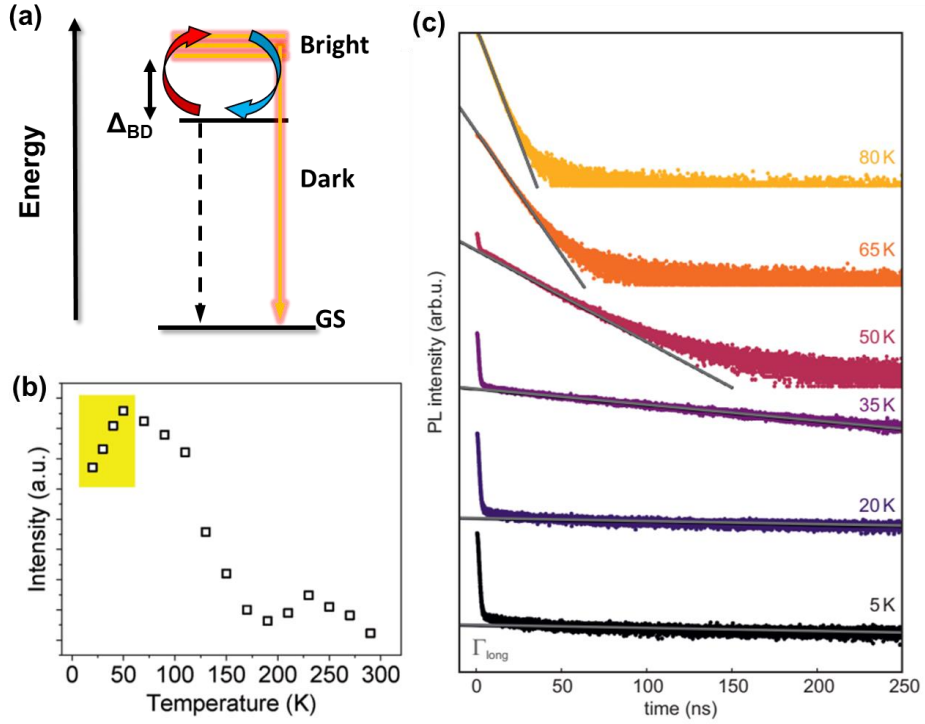

Fig. 3. (a) Schematic of excitons energy levels, recombination and scattering paths between exciton states (the splitting of the bright state is neglected). (b) dependence of PL intensity as a function of temperature for $(BA)_2PbI_4$ (BA stands for butylammonium). (c) Temperature-dependent PL decay traces between 5 and 80 K for n=4 $Cs_{n-1}Pb_nBr_{3n+1}$ nanoplatelets. Panels (b) and (c) reprinted with permission from [52] and [54] respectively.

Many of the attempts to extract bright-dark states were based on photoluminescence (PL) studies [49,50,52,54]. In this type of experiment, the splitting between optically inactive and optically active bright states is extracted from the temperature-dependent evolution of PL intensity and PL dynamics. This is an indirect approach where the energy difference between optically active and inactive levels is determined by modelling the PL intensity and dynamics as a function of temperature assuming thermal activation from dark to bright states [42,54-57] as schematical shown in Figure 3a. If the dark state is the lowest-lying state it is expected that with increasing temperature the PL intensity will rise (see a yellow rectangle in Figure 3b). Simultaneously at the lowest temperature, the PL signal is dominated by the fast decay due to the relaxation of excitons to an optically inactive dark state and eventually weak long-living component being a hallmark of weakly efficient back-scattering of excitons from dark to the bright state. With the rise of temperature, the dominating part of PL decay

elongates since the excitons in a dark state are more and more effectively activated to the bright state. In this way, the long-living dark state contributes more to the PL decay signal (see Figure 3c). Such PL behaviour was observed for different 2D perovskites [49,50,52,54]. However, such an approach provides only a rough estimation of the splitting since PL behaviour can be additionally affected by trap states and thermally activated nonradiative recombination processes as indicated by the non-monotonic behaviour of PL intensity with the temperature as visible in Figure 3b. Nevertheless, determined with this approach bright dark state splitting is in the range of several meV (Table 2). This is significantly more than in other QW or quantum dots systems [36,37,42,51] pointing out that extreme enhancement of excitonic effects in 2D perovskites leads to extreme bright-dark exciton state splitting, one or two orders of magnitude larger than in many other semiconductor material systems.

Much more reliable results can be obtained if the energy of the dark exciton state can be measured directly. A simple solution is based on exploiting an external magnetic field which brightens the dark state, facilitating its direct observation by optical spectroscopy methods. Such an approach has been extensively exploited in the case of different nanocrystals and epitaxial quantum dots [37,42,56]. However, for 2D perovskites where splitting between the bright and dark states is expected to be significant, a particularly strong magnetic field is needed to mix bright and dark excitonic states. Therefore only very recently with the magnetic field as high as 65T direct measurements of the dark exciton in 2D perovskites has been successful [47,53].

When the magnetic field is on, the intrinsic symmetry of the crystal is broken and as a result, bright and dark exciton states mix with each other. Still, the magnetic field-induced states can be expressed as a linear combination of states without a magnetic field. The way how the exciton states mix with each other depends on the relative orientation of magnetic field **B**, light wave vector **k** and crystal **c** axis orientation [37,45,58].

In Faraday geometry, where **B**||**k**||**c**, the magnetic field lifts the degeneracy of the bright in-plane states and mixes the dark state with the out-of-plane dipole moment state (Z state). In the so-called Voigt geometry where **B**⊥**k**||**c** dark and out of plane state mixes with both in-plane exciton states in such a way that brightened dark state has transition dipole oriented along the magnetic field (longitudinal states) while out of plane state became visible for the light polarization perpendicular to the **B** (transverse state)**.** The exciton states mixing is schematically presented in Figure 4. The detailed formulas describing the evolution of each state in a magnetic field can be found in ref. [45,47,58]. It is worth noting that mixed states are perfectly parallel (or perpendicular) to magnetic field only when the two in-

plane states are degenerate. When two bright in-plane exciton states are not degenerate the polarization of states mixed by magnetic field is in principle slightly tilted from direction of the field.

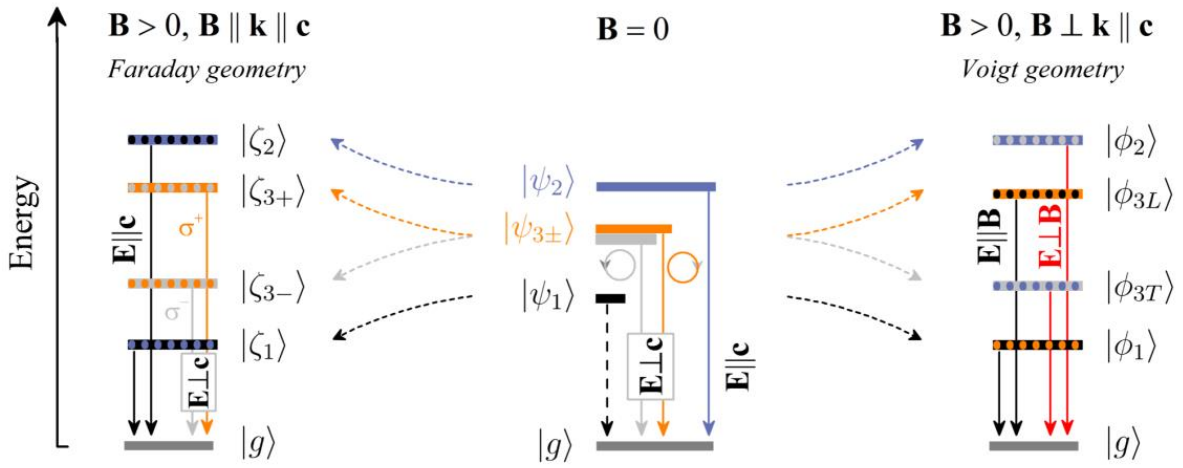

Fig. 4. Schematic representation of different configurations of excitons levels when the magnetic field is on for Faraday (left) and Voigt (right) geometry. **E** is a light electric field vector.

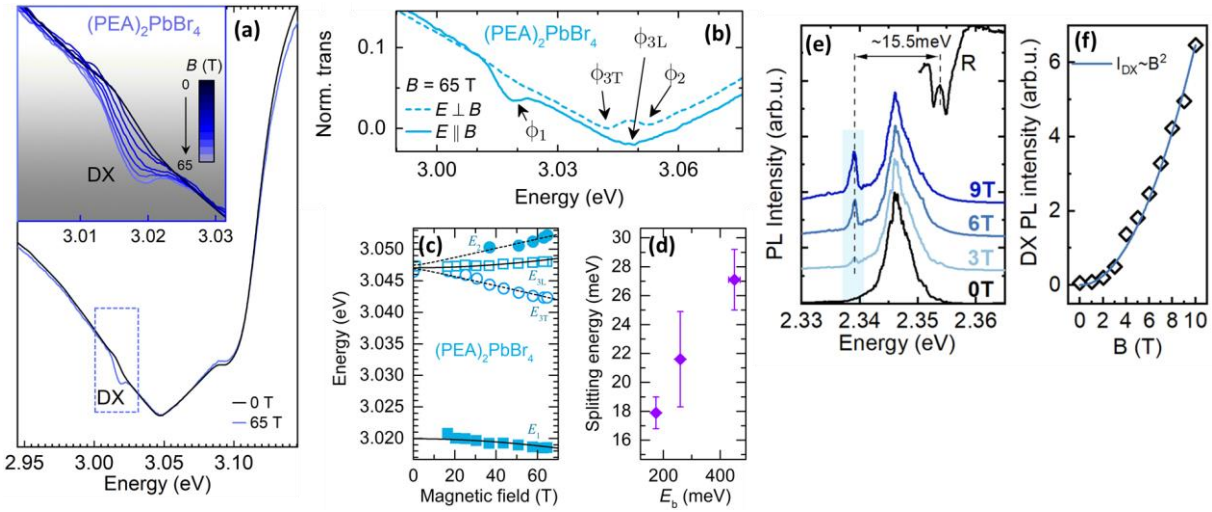

Fig. 5. (a) Spectra of $(PEA)_2PbBr_4$ measured at zero magnetic fields (black) and at B = 65 T (coloured lines). Transmission in the low-energy region indicated by the dashed rectangle shows the appearance of the brightened dark exciton (DX) transition at a high magnetic field. (b) Transmission spectra measured at a magnetic field of B = 65 T, with the excitation light polarized along and normal to the magnetic field B. (c) Evolution of transition energy for all four excitonic states in a magnetic field for the $(PEA)_2PbBr_4$. (d) Bright-dark energy splitting at B = 0 T vs exciton binding energy. (e) PL spectra of $(PEA)_2PbI_4$ measured under different magnetic fields. The shading indicates the position of the brightened dark state. (f) Dark exciton transition PL intensity versus magnetic field showing quadratic dependence for $(PEA)_2PbI_4$. Panels (a)-(d) are reprinted from [47]. Panels (e) and (f) reprinted with permission from [53] Copyright 2022 American Chemical Society.

In the work [47] with the use of a magnetic field up to 65T the brightening of the dark state in Voigt configuration was observed for $(PEA)_2SnI_4$, $(PEA)_2PbI_4$, $(PEA)_2PbBr_4$ 2D perovskites where PEA stand for phenylethylamine. As shown in Figure 5a applied magnetic field resulted in a new spectral feature visible on the low energy side which was attributed to the brightened dark state. The polarization resolved studies (see Figure 5b) allowed to track the evolution of all 4 excitonic states in a magnetic field (see Figure 5c) and with the use of appropriate fitting to extract the energy of the dark state at 0T field. According to the expected selection rules [45,59] the dark state was observed only when the electric field of the light was parallel to the magnetic field and in perpendicular configuration the hallmark of the out-of-plane state was visible. Studies performed for three different chemical compositions of 2D perovskites allowed for observation of how bright-dark state splitting evolves with exciton binding energy. Bright-dark states splitting at 0T field increase from 18 meV for $(PEA)_2SnI_4$ up to almost 30 meV for $(PEA)PbBr_4$ i.e. increase with increasing exciton binding energy which is summarized in Figure 5d.

The above investigations consider only the simplest form of 2D perovskites with thickness n=1. So far there are not too many studies regarding the dependence of bright-dark state splitting as a function of 2D perovskite quantum well thickness. The only systematic work was performed on $Cs_{n-1}Pb_nBr_{3n+1}$ nanoplatelets [54], which can be considered as a form of 2D Rudlesden-Popper perovskites. In this work, the authors performed experimental and theoretical studies and concluded that bright-dark state splitting changes from about 32 meV for nanoplatelets of thickness n=2 to around 2 meV for nanoplatelets of thickness n=8. Again this trend follows the expectation that bright-dark state splitting decreases with decreasing exciton binding energy. It can be also noticed that despite the thinnest sample being n=2 the bright dark splitting is very close to $(PEA)_2PbBr_4$ (n=1) which can be related to different organic spacer used in the case of nanoplatelets namely oleylamine instead of PEA and/or to the influence of lateral confinement due to finite size of nanoplatelets.

Recently also the observation of the dark states in Faraday configuration was reported for $(PEA)_2PbI_4$, single crystals [53]. Thanks to the use of a high numerical aperture objective it was possible to see PL emission from the dark state (see Figure 5e) even though it gains oscillator strength from the out-of-plane bright state [45,58,59]. The origin of this PL emission was corroborated by its increasing quadratically intensity (see Figure 5f). Interestingly the extracted in this study bright dark state splitting was close but clearly lower

than those extracted in the absorption studies in Voigt configuration [47] (~16meV and 22meV respectively).

Bright exciton fine structure

As we mentioned above the degeneracy of the bright states can be also lifted depending on the symmetry of the system. The structure of the bright states is also a subject of ongoing discussions. For example, in the ladder of excitonic states presented in Figure 2, we place the out-of-plane state above the in-plane bright states after [47]. However, there are reports that suggest that the *Z* state is below bright in-plane states [48,60,61], like in 3D perovskites [40] or that its position depends on 2D perovskite QW thickness [54]. Also, some controversy appears regarding the in-plane exciton states splitting. For example $(PEA)_2PbI_4$ possesses two inequivalent *x* and *y* axes [62]. Therefore, it is expected that the degeneracy of the in-plane states is lifted. Indeed, polarization-resolved PL studies show splitting of the in-plane states of around 2 meV (see Figure 6a). However, the reported number of transitions observed in photoluminescence [46] (PL), ascribed to bright in-plane excitonic transitions [46,63] was larger than two which is in obvious contradiction to band-structure analysis. In contrast, very recent results of polarization-resolved reflectance spectra show only two in-plane bright state transitions [53] with perpendicular dipole orientation as shown in Figure 6b and 6c. In the same work, it was proposed that the multiple peak structure of PL emission spectra is related to the exciton-polaron emission which derives from the bright in-plane state preserving their selection rules. Such interpretation is in agreement with theoretical predictions [45,59] and explains the origin of additional PL signals. As shown in Figure 6d the dominating PL band is redshifted with respect to excitonic transitions visible in reflectance spectra which is related to the reconfiguration of the soft and the ionic perovskite lattice [64-67] which dress the free exciton states, leading to a complex PL response. The free excitonic transition in PL manifests only as weak features on the high-energy side of the spectra.

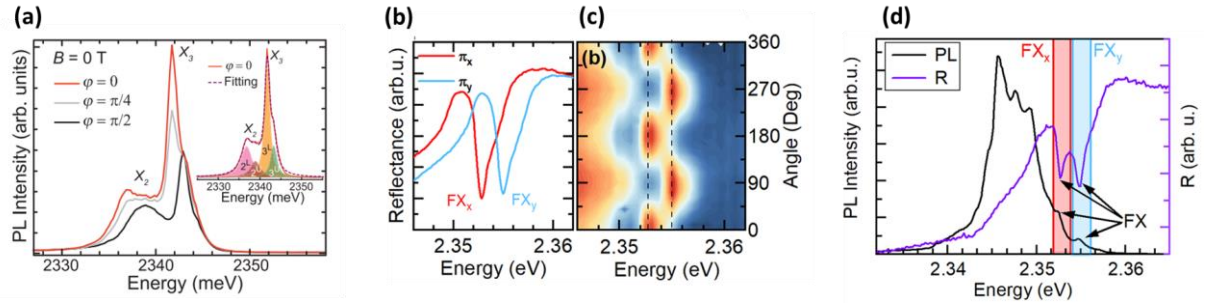

Fig. 6 (a) Linearly polarized PL spectra form $(PEA)_2PbI_4$. (b) The reflectance spectrum of $(PEA)_2PbI_4$ measured in two orthogonal linear polarizations showing clear splitting and only two in-plane exciton

states. (c) Full dependence of reflectance spectrum versus polarization angle for $(PEA)_2PbI_4$. (d) PL (black) and reflectance (violet) response of (PEA)2PbI4; the shaded areas indicate the contribution of two in-plane free excitonic transitions to PL response. Panel (a) reprinted with permission from [46] Copyright 2020 American Chemical Society, Panels (b),(c) and (d) reprinted with permission from [53] Copyright 2022 American Chemical Society.

Discussion and Outlook

The exciton fine structure is not unique to perovskites as it is observed for excitons in any semiconductor. However, what is unique about it is its huge magnitudes which put important questions about how its presence affects the properties of these materials. The particularly large dark-bright splitting in the range of a few tens of meV [47-50,68] should make us think how it is possible that 2D perovskites are so good light emitters even at cryogenic temperatures (PL efficiency in the range of few tens of percent's [10]). Enhanced bright-dark state splitting should reduce device efficiency due to dominant occupation of the ground, not emissive, state at thermal equilibrium [37,42]. Therefore the understanding of the excitonic properties of 2D materials is not only a matter of scientific curiosity but might shape deterministic development strategies to enhance the operational parameters of future optoelectronic devices. In fact, such an intense PL emission at low temperatures indicates that the thermalization dynamic between bright and dark excitons is considerably slowed down resulting in a hot, non-thermal distribution of excitons which was partially corroborated by the magneto-optical studies [47]. The analysis of the thermal occupation factor and oscillator strength revealed that the exciton population temperature is around 35 K higher than the lattice temperature. However, a detailed understanding of the mechanism standing behind this hot emission is still missing.

One of the explanations proposed during recent years joins superior light emission efficiency with the mechanical properties of perovskite crystals [1,42,69]. The softness of perovskites (including their bulk and lower dimensional forms) is one of the most striking features, which distinguish them from epitaxial semiconductors. The bulk moduli characterizing 3D and 2D perovskites are around ten times lower than the one describing silicon or gallium arsenide [70,71]. The soft lattice results in a specific exciton-phonon interaction in perovskite materials, in particular, excitons are known to couple very weakly to acoustic phonons, while they show a strong coupling to optical phonon modes [42,69,72,73]. It was proposed that in the case of perovskites nanocrystals this leads to extremely reduced phonon-assisted relaxation into dark exciton states, due to a mismatch between bright-dark state splitting and optical phonon energy as schematically shown in Figure 7.

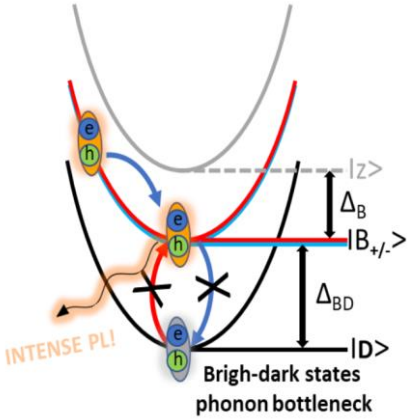

Fig.7 Scheme of exciton fine structure in 2D perovskites. The weak exciton-acoustic phonon coupling, together with the mismatch between optical phonon and bright-dark exciton splitting can lead to a phonon bottleneck.

Unfortunately, the phonon bottleneck effect has been studied mainly in perovskite nanocrystals [42,69] which share a soft lattice with 2D perovskites but at the same time, the density of states are different in these two material systems. Therefore the extrapolation of these conclusions from one material system to the other has to be done with special attention requiring intensive studies in the field of microscopic modelling (understood as a modelling of exciton dynamics that takes in to account all possible scattering process of relaxing excitons) and experimental studies to corroborate the phonon bottleneck hypothesis. Nevertheless, it has to be noted that the correlation between vibration and emission properties was also observed for 2D perovskites [10,21]. Yet clear evidence for the phonon bottleneck between bright and dark exciton states in 2D perovskites was not presented. If the discussed hypothesis is true then 2D perovskites constitute an unprecedented playground to study the phonon bottleneck between bright and dark exciton states as they offer the possibility for independent modification of the excitonic fine structure by playing with the QW thickness and the phonon spectrum with the use of organic spacer [10,21,24,33,72,74]. This provides an opportunity to control phonon bottleneck for a deterministic design of novel highly efficient light emitters or solar cells.

It is important to stress that so far in this review we neglect the polaronic character of metal-halide perovskites since the exciton fine structure seems to be quite well described with the standard semiconductor theory. However, there are reports suggesting that the polaronic nature of perovskites is crucial to properly address this aspect [66,75,76]. Indeed ones have to be aware that in general, description neglecting carrier interaction with the lattice in perovskites is a significant simplification. As we mentioned, the softness of perovskite crystals results in low energy phonon modes. This together with significant

contrast between static and optical frequency dielectric screening, characteristic for ionic crystals, promote strong carrier lattice interaction. Therefore dressing of carriers and excitons with a lattice deformation should be taken in to account in the Hamiltonian of the system to reveal how the properties of electrons, holes and excitons renormalize due to lattice dynamics [1,14,15,75,77]. Moreover the presence of large-amplitude anharmonic vibrations [21] at higher temperatures also can have nontrivial impact on the carriers and excitons in these material system. These large lattice motions can stabilize localized electronic excited states and are likely to reduce the charge carrier mobility of the materials [77-79]. It is important to note that there are several indirect experimental evidence pointing on crucial role of exciton-lattice coupling in these materials however there is still a need of experimental and theoretical development to directly probe unambiguously exciton-polarons in 2D perovskites [66,75,76]. The knowledge about exciton-phonon coupling is certainly crucial to describe the phonon-bottleneck effect however it seems also to be crucial to address such fundamental aspects as a proper description of electron and hole interaction in these materials [80-83]. While all these aspects are more and more intensively investigated in the case of 3D [80,84,85] perovskites for the 2D perovskites we are just at the beginning of these studies [75,86].

Conclusions

In this article we have reviewed the recent progress in understanding the exciton FSS in 2D metal-halide perovskites. As we have shown there is still ongoing debate about the precise quantification of the exciton state leader. Nevertheless, most of the recent experimental reports seams to collaborate that bright-dark exciton states splitting is in the range of several to few tens of meV in thinnest 2D perovskites quantum wells and that the degeneracy of the in-plane exciton states is lifted. Despite the significant progress made in this field in recent years, still many questions await precise answers. Very little is known about the evolution of exciton fine structure with quantum well thickness in this materials system. It is not clear what is the detailed mechanism related to very efficient light emission from 2D perovskites having in mind the extreme splitting of bright and dark states. It is very interesting to know if the possible phonon bottleneck effect can be controlled with the independent tuning of exciton states splitting and phonon spectrum. This would provide an opportunity not only to thoroughly understand phonon-mediated relaxation between bright and dark exciton states but also to control phonon bottleneck for a deterministic design of novel highly efficient light emitters.

Acknowledgements

This work was funded by National Science Centre Poland within the SONATA (2021/43/D/ST3/01444)

References

[1] Egger, D. A.; Bera, A.; Cahen, D.; Hodes, G.; Kirchartz, T.; Kronik, L.; Lovrincic, R.; Rappe, A.M.; Reichman, D.R.; Yaffe, O.; What remains unexplained about the properties of halide Perovskites?. *Adv. Mater.* **2018**, 30, 1800691. DOI: 10.1002/adma.201800691

[2] Stranks, S.D.; Eperon, G.E.; Grancini, G.; Menelaou, C.; Alcocer, M.J.; Leijtens, T.; Herz, L.M.; Petrozza, A.; Snaith, H.J.; Electron-hole diffusion lengths exceeding 1 micrometer in an organometal trihalide perovskite absorber. *Science* **2013**, 342, 341-344. DOI: 10.1126/science.1243982

[3] Huang, J.; Yuan, Y.; Shao, Y.; Yan, Y.; Understanding the physical properties of hybrid perovskites for photovoltaic applications. *Nat. Rev. Mater.* **2017**, 2, 17042. DOI: 10.1038/natrevmats.2017.42

[4] Kang, J.; Wang, L.-W.; High defect tolerance in lead halide perovskite $CsPbBr_3$. *J. Phys. Chem. Lett.* **2017**, 8, 489-493. DOI: 10.1021/acs.jpclett.6b02800

[5] Huang, H.; Bodnarchuk, M.I.; Kershaw, S.V.; Kovalenko, M.V.; Rogach, A.L.; Lead halide perovskite nanocrystals in the research spotlight: Stability and defect tolerance. *ACS Energy Lett.* **2017**, 2, 2071-2083. DOI: 10.1021/acsenergylett.7b00547

[6] Tsai, H.; Nie, W.; Blancon, J.C.; Stoumpos, C.C.; Asadpour, R.; Harutyunyan, B.; Neukirch, A.J.; Verduzco, R.; Crochet, J.J.; Tretiak, S.; et al. High-efficiency two-dimensional ruddlesden-popper perovskite solar cells. *Nature* **2016**, 536, 312-316. DOI: 10.1038/nature18306

[7] Chen, Y.; Sun, Y.; Peng, J.; Tang, J.; Zheng, K.; Liang, Z.; 2D Ruddlesdene-Popper perovskites for optoelectronics. *Adv. Mater.* **2018**, 30, 1703487. DOI: 10.1002/adma.201703487

[8] Blancon, J.C.; Tsai, H.; Nie, W.; Stoumpos, C.C.; Pedesseau, L.; Katan, C.; Kepenekian, M.; Soe, C.M.M.; Appavoo, K.; Sfeir, M.Y.; et al. Extremely efficient internal exciton dissociation through edge states in layered 2D perovskites. *Science* **2017**, 355, 1288–1291. DOI: 10.1126/science.aal421

[9] Cao, D.H.; Stoumpos, C.C.; Farha, O.K.; Hupp, J.T.; Kanatzidis, M.G.; 2D homologous perovskites as light-absorbing materials for solar cell applications. *J. Am. Chem. Soc.* **2015**, 137, 7843-7850. DOI: 10.1021/jacs.5b03796

[10] Gong, X.; Voznyy, O.; Jain, A.; Liu, W.; Sabatini, R.; Piontkowski, Z.; Walters, G.; Bappi, G.; Nokhrin, S.; Bushuyev, O.; et al. Electron–phonon interaction in efficient perovskite blue emitters. *Nat. Mater.* **2018**, 17, 550-556. DOI: 10.1038/s41563-018-0081-x

[11] Straus, D.B.; Kagan, C.R.; Electrons, excitons, and phonons in two-dimensional hybrid perovskites: connecting structural, optical, and electronic properties. *J. Phys. Chem. Lett.* **2018**, 9, 1434-1447. DOI: 10.1021/acs.jpclett.8b00201

[12] Mao, L.; Ke, W.; Pedesseau, L.; Wu, Y.; Katan, C.; Even, J.; Wasielewski, M.R.; Stoumpos, C.C.; Kanatzidis, M.G.; hybrid dion–jacobson 2d lead iodide perovskites. *J. Am. Chem. Soc.* **2018**, 140, 3775-3783. DOI: 10.1021/jacs.8b00542

[13] Smith, M.D.; Karunadasa, H.I.; White-light emission from layered halide perovskites. *Acc. Chem. Res.* **2018**, 51, 619-627. DOI: 10.1021/acs.accounts.7b00433

[14] Schilcher, M.J.; Robinson, P.J.; Abramovitch, D.J.; Tan, L.Z.; Rappe, A.M.; Reichman, D.R.; Egger, D.A.; The significance of polarons and dynamic disorder in halide perovskites. *ACS Energy Lett.* **2021**, 6, 2162-2173. DOI: 10.1021/acsenergylett.1c00506

[15] Sendner, M.; Nayak, P.K.; Egger, D.A.; Beck, S.; Müller, C.; Epding, B.; Kowalsky, W.; Kronik, L.; Snaith, H.J.; Pucci, A.; Lovrinčić, R.; Optical phonons in methylammonium lead halide perovskites and implications for charge transport. *Mater. Horizons* **2016**, 3, 613-620. DOI: 10.1039/C6MH00275G

[16] Paritmongkol, W.; Dahod, N.S.; Stollmann, A.; Mao, N.; Settens, C.; Zheng, S.; Tisdale, W.A.; Synthetic variation and structural trends in layered two-dimensional alkylammonium lead halide perovskites. *Chem. Mater.* **2019**, 31, 5592-5607. DOI: 10.1021/acs.chemmater.9b01318

[17] Dyksik, M.; Wang, S.; Paritmongkol, W.; Maude, D.K.; Tisdale, W.A.; Baranowski, M.; Plochocka, P.; Tuning the excitonic properties of the 2D $(PEA)_2(MA)_{n-1}Pb_nI_{3n+1}$ perovskite family via quantum confinement. *J. Phys. Chem. Lett.* **2021**, 12, 1638-1643. DOI: 10.1021/acs.jpclett.0c03731

[18] Blancon, J.C.; Stier, A.V.; Tsai, H.; Nie, W.; Stoumpos, C.C.; Traore, B.; Pedesseau, L.; Kepenekian, M.; Katsutani, F.; Noe, G.T.; et al. Scaling law for excitons in 2D perovskite quantum wells. *Nat. Commun.* **2018**, 9, 2254. DOI:10.1038/s41467-018-04659-x

[19] Du, K.Z.; Tu, Q.; Zhang, X.; Han, Q.; Liu, J.; Zauscher, S.; Mitzi, D.B.; Two-dimensional lead(II) halide-based hybrid perovskites templated by acene alkylamines: Crystal structures, optical properties, and piezoelectricity. *Inorg. Chem.* **2017**, 56, 9291-9302. DOI: 10.1021/acs.inorgchem.7b01094

[20] Knutson, J.L.; Martin, J.D.; Mitzi, D.B.; Tuning the band gap in hybrid tin iodide perovskite semiconductors using structural templating. *Inorg. Chem.* **2005**, 44, 4699-4705.
DOI: 10.1021/ic050244q

[21] Menahem, M.; Dai, Z.; Aharon, S.; Sharma, R.; Asher, M.; Diskin-Posner, Y.; Korobko, R.; Rappe, A.M.; Yaffe, O.; Strongly anharmonic octahedral tilting in two-dimensional hybrid halide perovskites. *ACS Nano* **2021**, 15, 10153-10162. DOI: 10.1021/acsnano.1c02022

[22] Dyksik, M.; Duim, H.; Zhu, X.; Yang, Z.; Gen, M.; Kohama, Y.; Adjokatse, S.; Maude, D.K.; Loi, M.A.; Egger, D.A.; et al. Broad tunability of carrier effective masses in two-dimensional halide perovskites. *ACS Energy Lett.* **2020**, 5, 3609-3616.
DOI: 10.1021/acsenergylett.0c01758

[23] Pedesseau, L.; Sapori, D.; Traore, B.; Robles, R.; Fang, H.-H.; Loi, M.A.; Tsai, H.; Nie, W.; Blancon, J.-C.; Neukirch, A.; et al. Advances and promises of layered halide hybrid perovskite semiconductors. *ACS Nano* **2016**, 10, 9776-9786. DOI: 10.1021/acsnano.6b05944

[24] Straus, D.B.; Hurtado Parra, S.; Iotov, N.; Zhao, Q.; Gau, M.R.; Carroll, P.J.; Kikkawa, J.M.; Kagan, C.R.; Tailoring hot exciton dynamics in 2D hybrid perovskites through cation modification. *ACS Nano* **2020**, 14, 3621-3629 DOI: 10.1021/acsnano.0c00037

[25] Passarelli, J.V.; Mauck, C.M.; Winslow, S.W.; Perkinson, C.F.; Bard, J.C.; Sai, H.; Williams, K.W.; Narayanan, A.; Fairfield, D.J.; Hendricks, M.P.; et al. Tunable exciton binding energy in 2D hybrid layered perovskites through donor–acceptor interactions within the organic layer. *Nat. Chem.* **2020**, 12, 672-682. DOI: 10.1038/s41557-020-0488-2

[26] Katan, C.; Mercier, N.; Even, J.; Quantum and dielectric confinement effects in lower-dimensional hybrid perovskite semiconductors. *Chem. Rev.* **2019**, 119, 3140-3192.
DOI: 10.1021/acs.chemrev.8b00417

[27] Gippius, N.A.; Muljarov, E.A.; Tikhodeev, S.G.; Ishihara, T.; Keldysh, L.V.; Dielectrically confined excitons and polaritons in natural superlattices–perovskite lead iodide semiconductors. *MRS Online Proceedings Library* **1993**, 328, 775-780.
DOI: 10.1557/PROC-328-775

[28] Ishihara, T.; Hong, X.; Ding, J.; Nurmikko, A.; Dielectric confinement effect for exciton and biexciton states in PbI_4-based two-dimensional semiconductor structures. *Surf. Sci.* **1992**, 267, 323-326. DOI: 10.1016/0039-6028(92)91147-4

[29] Hong, X.; Ishihara, T.; Nurmikko, A.V.; Dielectric confinement effects on excitons in PbI_4-based layered semiconductors. *Phys. Rev. B* **1992**, 45, 6961-6964. DOI: 10.1103/PHYSREVB.45.6961

[30] Tanaka, K.; Takahashi, T.; Kondo, T.; Umeda, K.; Ema, K.; Umebayashi, T.; Asai, K.; Uchida, K.; Miura, N.; Electronic and excitonic structures of inorganic–organic perovskite-type quantum-well crystal $(C_4H_9NH_3)_2PbBr_4$. *Jpn. J. Appl. Phys.* **2005**, 44, 5923. DOI: 10.1143/JJAP.44.5923

[31] Yaffe, O.; Chernikov, A.; Norman, Z.M.; Zhong, Y.; Velauthapillai, A.; van der Zande, A.; Owen, J.S.; Heinz, T.F.; Excitons in ultrathin organic-inorganic perovskite crystals. *Phys. Rev.* **2015**, 92, 045414. DOI: 10.1103/PhysRevB.92.045414

[32] Cheng, B.; Li, T.; Maity, P.; Wei, P.; Nordlund, D.; Ho, K.; Lien, D.; Miao, X.; et al. Extremely reduced dielectric confinement in two-dimensional hybrid perovskites with large polar organics.; *Commun. Phys.* **2018**, 1, 80. DOI: 10.1038/s42005-018-0082-8

[33] Straus, D.B.; Hurtado Parra, S.; Iotov, N.; Gebhardt, J.; Rappe, A.M.; Subotnik, J.E.; Kikkawa, J.M.; Kagan, C.R.; Direct observation of electron-phonon coupling and slow vibrational relaxation in organic-inorganic hybrid perovskites. *J. Am. Chem. Soc.* **2016**, 138, 13798-13801. DOI: 10.1021/jacs.6b08175

[34] Gauthron, K.; Lauret, J.; Doyennette, L.; Lanty, G.; Al Choueiry, A.; Zhang, S.J.; Largeau, L.; Mauguin, O.; Bloch, J.; Deleporte, E.; Optical spectroscopy of two-dimensional layered $(C_6H_5C_2H_4\text{-}NH_3)_2\text{-}PbI_4$ *perovskite. Opt. Express* **2010**, 18, 5912-5919. DOI: 10.1364/OE.18.005912

[35] Gélvez-Rueda, M.C.; Hutter, E.M.; Cao, D.H.; Renaud, N.; Stoumpos, C.C.; Hupp, J.T.; Savenije, T.J.; Kanatzidis, M.G.; Grozema, F.C.; Interconversion between free charges and bound excitons in 2D hybrid lead halide perovskites. *J. Phys. Chem. C* **2017**, 121, 26566-26574. DOI: 10.1021/acs.jpcc.7b10705

[36] Fu, H.; Wang, L.; Zunger, A.; Excitonic exchange splitting in bulk semiconductors. *Phys. Rev. B* **1999**, 59, 5568-5574. DOI: 10.1103/PhysRevB.59.5568

[37] Bayer, M.; Ortner, G.; Stern, O.; Kuther, A.; Gorbunov, A.A.; Forchel, A.; Hawrylak, P.; Fafard, S.; Hinzer, K.; Reinecke, T.L.; et al. Fine structure of neutral and charged excitons in self-assembled In(Ga)As/(Al)GaAs quantum dots. *Phys. Rev. B* **2002**, 65, 195315. DOI: 10.1103/PhysRevB.65.195315

[38] Fu, M.; Tamarat, P.; Huang, H.; Even, J.; Rogach, A.L.; Lounis, B.; Neutral and charged exciton fine structure in single lead halide perovskite nanocrystals revealed by magneto–optical spectroscopy. *Nano Lett.* **2017**, 17, 2895-2901. DOI: 10.1021/acs.nanolett.7b00064

[39] Sercel, P.C.; Lyons, J.L.; Wickramaratne, D.; Vaxenburg, R.; Bernstein, N.; Efros, A.L.; Exciton fine structure in perovskite nanocrystals. *Nano Lett.* **2019**, 19, 4068-4077. DOI: 10.1021/acs.nanolett.9b01467

[40] Ramade, J.; Andriambariarijaona, L.M.; Steinmetz, V.; Goubet, N.; Legrand, L.; Barisien, T.; Bernardot, F.; Testelin, C.; Lhuillier, E.; Bramati, A.; et al. Fine structure of excitons and electron–hole exchange energy in polymorphic CsPbBr3 single nanocrystals. *Nanoscale* **2018**, 10, 6393-6401. DOI: 10.1039/C7NR09334A

[41] Becker, M.A.; Vaxenburg, R.; Nedelcu, G.; Sercel, P.C.; Shabaev, A.; Mehl, M.J.; Michopoulos, J.G.; Lambrakos, S.G.; Bernstein, N.; Lyons, J.L.; et al. Bright triplet excitons in caesium lead halide perovskites. *Nature* **2018**, 553, 189. DOI: 10.1038/nature25147

[42] Tamarat, P.; Bodnarchuk, M.I.; Trebbia, J.-B.; Erni, R.; Kovalenko, M.V.; Even, J.; Lounis, B.; The ground exciton state of formamidinium lead bromide perovskite nanocrystals is a singlet dark state. *Nat. Mater.* **2019**, 18, 717-724. DOI: 10.1038/s41563-019-0364-x

[43] Stevenson, R.M.; Young, R.J.; Atkinson, P.; Cooper, K.; Ritchie, D.A.; Shields, A.J.; A semiconductor source of triggered entangled photon pairs. *Nature* **2006**, 439, 179-182. DOI: 10.1038/nature04446

[44] Senellart, P.; Solomon, G.; White, A.; High-performance semiconductor quantum-dot single-photon sources. *Nat. Nanotechnol.* **2017**, 12, 1026-1039. DOI: 10.1038/nnano.2017.218

[45] Kataoka, T.; Kondo, T.; Ito, R.; Sasaki, S.; Uchida, K.; Miura, N.; Magneto-optical study on excitonic spectra in $(C_6H_{13}NH_3)_2PbI_4$. *Phys. Rev. B* **1993**, 47, 2010. DOI: 10.1103/PhysRevB.47.2010

[46] Do, T.T.H.; Del Aguila, A.G.; Zhang, D.; Xing, J.; Liu, S.; Prosnikov, M.A.; Gao, W.; Chang, K.; Christianen, P.C.M.; Xiong, Q.; Bright exciton fine-structure in two-dimensional lead halide perovskites. *Nano Lett.* **2020**, 20, 5141-5148. DOI: 10.1021/acs.nanolett.0c01364

[47] Dyksik, M.; Duim, H.; Maude, D.K.; Baranowski, M.; Loi, M.A.; Plochocka, P.; Brightening of dark excitons in 2D perovskites. *Sci. Adv.* **2021**, 7, 1-8. DOI: 10.1126/sciadv.abk0904

[48] Tanaka, K.; Takahashi, T.; Kondo, T.; Umeda, K.; Ema, K.; Umebayashi, T.; Asai, K.; Uchida, K.; Miura, N.; Electronic and excitonic structures of inorganic–organic perovskite-type quantum-well crystal $(C_4H_9NH_3)_2PbBr_4$. *Jpn. J. Appl. Phys.* **2005**, *44*, 5923.

DOI: 10.1143/jjap.44.5923

[49] Fang, H.; Yang, J.; Adjokatse, S.; Tekelenburg, E.; Kamminga, M.E.; Duim, H.; Loi, M.A.; Band-edge exciton fine structure and exciton recombination dynamics in single crystals of layered hybrid perovskites. *Adv. Funct. Mater.* **2019***,* 30, 6, 1907979. DOI: 10.1002/adfm.201907979

[50] Folpini, G.; Cortecchia, D.; Petrozza, A.; Srimath Kandada, A.R.R.; The role of dark exciton reservoir in the luminescence efficiency of two-dimensional tin halide perovskites. *J. Mater. Chem. C* **2020**, 8, 31, 10889-10896. DOI: 10.1039/d0tc01218a

[51] Blackwood, E.; Snelling, M.J.; Harley, R.T.; Andrews, S.R.; Foxon, C.T.; Exchange interaction of excitons in GaAs heterostructures. *Phys. Rev. B Condens. Matter* **1994**, 50, 19, 14246-14254. DOI: 10.1103/PhysRevB.50.14246

[52] Gan, Z.X.; Wen, X.M.; Zhou, C.H.; Chen, W.J.; Zheng, F.; Yang, S.; Davis, J.A.; Tapping, P.C.; Kee Tak, W.; Zhang, H.; et al. Transient energy reservoir in 2D perovskites. *Adv. Opt. Mater.* **2019**, 7, 1900971. DOI: 10.1002/adom.201900971

[53] Posmyk, K.; Zawadzka, N.; Dyksik, M.; Surrente, A.; Maude, D.K.; Kazimierczuk, T.; Babinski, A.; Molas, M.R.; Paritmongkol, W.; Maczka, M.; Tisdale, W.A.; Płochocka, P.; Baranowski, M.; Quantification of exciton fine structure splitting in a two-dimensional perovskite compound. *J. Phys. Chem. Lett*. **2022**, 13, 4463-4469. DOI: 10.1021/acs.jpclett.2c00942

[54] Gramlich, M.; Swift, M.W.; Lampe, C.; Lyons, J.L.; Döblinger, M.; Efros, A.L.; Sercel, P.C.; Urban, A.S.; Dark and bright excitons in halide perovskite nanoplatelets. *Adv. Sci.* **2021**, 9, 2103013. DOI: 10.29363/nanoge.incnc.2021.013

[55] Ramade, J.; Andriambariarijaona, L.M.; Steinmetz, V.; Goubet, N.; Legrand, L.; Barisien, T.; Bernardot, F.; Testelin, C.; Lhuillier, E.; Bramati, A.; et al. Fine structure of excitons and electron–hole exchange energy in polymorphic $CsPbBr_3$ single nanocrystals. *Nanoscale* **2018**, 10, 6393-6401. DOI: 10.1039/c7nr09334a

[56] Canneson, D.; Shornikova, E.V.; Yakovlev, D.R.; Rogge, T.; Mitioglu, A.A.; Ballottin, M.V.; Christianen, P.C.M.; Lhuillier, E.; Bayer, M.; Biadala, L.; Negatively charged and dark excitons in $CsPbBr_3$ perovskite nanocrystals revealed by high magnetic fields*. Nano Lett.* **2017**, 17, 6177-6183. DOI: 10.1021/acs.nanolett.7b02827

[57] Xu, K.; Vliem, J.F.; Meijerink, A.; Long-lived dark exciton emission in Mn-doped $CsPbCl_3$ perovskite nanocrystals. *J. Phys. Chem.* **2019**, 123, 979-984. DOI: 10.1021/acs.jpcc.8b12035

[58] Surrente, A.; Baranowski, M.; Plochocka, P.; Perspective on the physics of two-dimensional perovskites in high magnetic field. *Appl. Phys. Lett.* **2021**, 118, 170501

DOI: 10.1063/5.0048490

[59] Yu, Z.G.; Effective–mass model and magneto–optical properties in hybrid perovskites. *Sci. Rep.* **2016**, 6, 28576. DOI: 10.1038/srep28576

[60] Fieramosca, A.; De Marco, L.; Passoni, M.; Polimeno, L.; Rizzo, A.; Rosa, B.L.; Cruciani, G.; Dominici, L.; De Giorgi, M.; Gigli, G.; et al. Tunable out-of-plane excitons in 2D single-crystal perovskites. *ACS Photonics* **2018**, 5, 4179-4185. DOI: 10.1021/acsphotonics.8b00984

[61] Steger, M.; Janke, S. M.; Sercel, P.C.; Larson, B.W.; Lu, H.P.; Qin, X.X.; Yu, V.W.Z.; Blum, V.; Blackburn, J.L.; On the optical anisotropy in 2D metal-halide perovskites. *Nanoscale* **2022**, 14, 752-765. DOI: 10.1039/D1NR06899G

[62] Fang, H.H.; Yang, J.; Tao, S.; Adjokatse, S.; Kamminga, M.E.; Ye, J.; Blake, G.R.; Even, J.; Loi, M.A.; Unravelling light-induced degradation of layered perovskite crystals and design of efficient encapsulation for improved photostability. *Adv. Funct. Mater*. **2018**, 28, 1800305. DOI: 10.1002/adfm.201800305

[63] Neutzner, S.; Thouin, F.; Cortecchia, D.; Petrozza, A.; Silva, C.; Srimath Kandada, A.R.; Erratum: Exciton-polaron spectral structures in two-dimensional hybrid lead-halide perovskites. *Phys. Rev. Materials* **2018**, 4, 059901. DOI: 10.1103/physrevmaterials.4.059901

[64] Guo, Y.; Yaffe, O.; Hull, T.D.; Owen, J.S.; Reichman, D.R.; Brus, L.E.; Dynamic emission Stokes shift and liquid-like dielectric solvation of band edge carriers in lead-halide perovskites. *Nat. Commun.* **2019**, 10, 1175. DOI: 10.1038/s41467-019-09057-5

[65] Zhu, X.-Y.; V. Podzorov, V.; Charge carriers in hybrid organic-inorganic lead halide perovskites might be protected as large polarons. *J. Phys. Chem. Lett.* **2015**, 23, 4758-4761. DOI: 10.1021/acs.jpclett.5b02462

[66] Thouin, F.; Valverde-Chávez, D.A.; Quarti, C.; Cortecchia, D.; Bargigia, I.; Beljonne, D.; Petrozza, A.; Silva, C.; Kandada, A.R.S.; Phonon coherences reveal the polaronic character of excitons in two-dimensional lead halide perovskites. *Nat. Mater*. **2019**, 18, 349-356. DOI: 10.1038/s41563-018-0262-7

[67] Tao, W.; Zhang, C.; Zhou, Q.; Zhao, Y.; Zhu, H.; Momentarily trapped exciton polaron in two-dimensional lead halide perovskites. *Nat. Commun.* **2021**, 12, 1, 1400. DOI: 10.1038/s41467-021-21721-3

[68] Robert, C.; Amand, T.; Cadiz, F.; Lagarde, D.; Courtade, E.; Manca, M.; Taniguchi, T.; Watanabe, K.; Urbaszek, B.; Marie, X.; Fine structure and lifetime of dark excitons in transition metal dichalcogenide monolayers. *Phys. Rev. B* **2017**, 96, 155423. DOI: 10.1103/physrevb.96.155423

[69] Fu, M.; Tamarat, P.; Trebbia, J.B.; Bodnarchuk, M.I.; Kovalenko, M.V.; Even, J.;

Lounis, B.; Unraveling exciton–phonon coupling in individual $FAPbI_3$ nanocrystals emitting near–infrared single photons. *Nat. Commun.* **2018**, 9, 3318. DOI: 10.1038/s41467-018-05876-0

[70] Aguado, F.; Rodríguez, F.; Valiente, R.; Itiè, J.P.; Hanfland, M.; Pressure effects on Jahn-Teller distortion in perovskites: The roles of local and bulk compressibilities. *Phys. Rev. B* **2012**, 85, 100101. DOI: 10.1103/physrevb.85.100101

[71] Jaffe, A.; Lin, Y.; Karunadasa, H.I.; Halide perovskites under pressure: accessing new properties through lattice compression. *ACS Energy Lett.* **2017**, 2, 1549-1555. DOI: 10.1021/acsenergylett.7b00284

[72] Straus, D. B.; Iotov, N.; Gau, M. R.; Zhao, Q.; Carroll, P. J.; Kagan, C. R.; Longer cations increase energetic disorder in excitonic 2d hybrid perovskites. *J. Phys. Chem. Lett.* **2019**, 10, 1198-1205. DOI: 10.1021/acs.jpclett.9b00247

[73] Feldstein, D.; Perea-Causin, R.; Wang, S.; Dyksik, M.; Watanabe, K.; Taniguchi, T.; Plochocka, P.; Malic, E.; Microscopic picture of electron–phonon interaction in two-dimensional halide perovskites. *J. Phys. Chem. Lett.* **2020**, 11, 9975-9982. DOI: 10.1021/acs.jpclett.0c02661

[74] Mauck, C.M.; France-Lanord, A.; Hernandez Oendra, A.C.; Dahod, N.S.; Grossman, J.C.; Tisdale, W.A.; Inorganic cage motion dominates excited-state dynamics in 2D-layered perovskites $(C_xH_{2x\,1}NH_3)_2PbI_4$ (x = 4–9). *J. Phys. Chem.* **2019**, 123, 45, 27904-27916. DOI: 10.1021/acs.jpcc.9b07933

[75] Srimath Kandada, A.R.; Silva, C.; Exciton polarons in two-dimensional hybrid metal-halide perovskites. *J. Phys. Chem. Lett*. **2020**, 11, 3173-3184. DOI: 10.1021/acs.jpclett.9b02342

[76] Neutzner, S.; Thouin, F.; Cortecchia, D.; Petrozza, A.; Silva, C.; Kandada, A.R.S.; Exciton-polaron spectral structures in two-dimensional hybrid lead-halide perovskites. *Phys. Rev. Materials* **2018**, 6, 064605. DOI: 10.1103/physrevmaterials.2.064605

[77] Yin, J.; Li, H.; Cortecchia, D.; Soci, C.; Bredas, J.L.; Excitonic and polaronic properties of 2D hybrid organic–inorganic perovskites. *ACS Energy Lett.* **2017**, 2, 417-423. DOI: 10.1021/acsenergylett.6b00659

[78] Zhang, Z.; Fang, W.H.; Long, R.; Prezhdo, O.V.; Exciton dissociation and suppressed charge recombination at 2d perovskite edges: key roles of unsaturated halide bonds and thermal disorder. *J. Am. Chem. Soc.* **2019**, 141, 15557-15566. DOI: 10.1021/jacs.9b06046

[79] Sun, Q.; Zhao, C.; Yin, Z.; Wang, S.; Leng, J.; Tian W.; Jin, S.; Ultrafast and high-yield polaronic exciton dissociation in two-dimensional perovskites. *J. Am. Chem. Soc.* **2021**,

143, 19128-19136. DOI: 10.1021/jacs.1c08900

[80] Menéndez-Proupin, E.; Ríos, C.L.B.; Wahnón, P.; Nonhydrogenic exciton spectrum in perovskite $CH_3NH_3PbI_3$. *Phys. Status Solidi RRL* **2015**, 9, 559-563. DOI: 10.1002/pssr.201510265

[81] Pollmann, J.; Büttner, H.; Effective Hamiltonians and bindings energies of Wannier excitons in polar semiconductors. *Phys. Rev. B* **1977**, 16, 4480. DOI: 10.1103/PhysRevB.16.4480

[82] Haken, H.; Die theorie des exzitons im festen Körper. *Fortschr. Phys.* **1958**, 6, 271-334. DOI: 10.1002/prop.19580060602

[83] Bajaj, K.K.; Effect of electron-phonon interaction on the binding energy of a Wannier exciton in a polarizable medium. *Solid State Commun.* **1974**, 15, 1221-1224. DOI: 10.1016/0038-1098(74)90055-6

[84] Filip, M.R.; Haber, J.B.; Neaton, J.B.; Phonon screening of excitons in semiconductors: halide perovskites and beyond. *Phys. Rev. Lett.* **2021**, 127, 067401. DOI: 10.1103/physrevlett.127.067401

[85] Baranowski, M.; Plochocka, P.; Excitons in metal-halide perovskites. *Adv. Energy Mater.* **2020**, 10, 1903659. DOI: 10.1002/aenm.201903659

[86] Filip, M.R.; Qiu, D.Y.; Del Ben M.; Neaton, J.B.; Screening of excitons by organic cations in quasi-two-dimensional organic–inorganic lead-halide perovskites. *Nano Lett.* **2022**, 22, 4870-4878 DOI: 10.1021/acs.nanolett.2c01306

Copyright: © 2022 by the authors. Submitted for possible open access publication under the terms and conditions of the Creative Commons Attribution (CC BY) license (https://creativecommons.org/licenses/by/4.0/).